Journal of Cellular Biochemistry 103:1379–1393 (2008)

Calcium Oxalate Crystals in Fetal Bovine Serum: Implications for Cell Culture, Phagocytosis and Biomineralization Studies In Vitro

Claudio E. Pedraza,[1] Yung-Ching Chien,[1] and Marc D. McKee[1,2]*

[1]Faculty of Dentistry, McGill University, Montreal, Quebec, Canada H3A 2B2
[2]Department of Anatomy and Cell Biology, McGill University, Montreal, Quebec, Canada H3A 2B2

Abstract Cell culture methods and models are key investigative tools for cell and molecular biology studies. Fetal bovine serum (FBS) is commonly used as an additive during cell culture since its constituents promote cell survival, proliferation and differentiation. Here we report that commercially available FBS from different major suppliers consistently contain precipitated, calcium oxalate crystals—either in the monohydrate (COM) or dihydrate (COD) form. Mineral structure and phase identification of the crystals were determined by X-ray diffraction, chemical composition by energy-dispersive X-ray microanalysis, and imaging and measurement of crystal growth steps by atomic force microscopy—all identified and confirmed crystallographic parameters for COM and COD. Proteins binding to the crystals were identified by immunoblotting, revealing the presence of osteopontin and fetuin-A (α_2HS-glycoprotein)—known regulators of crystal growth found in serum. Macrophage cell cultures exposed to calcium oxalate crystals showed internalization of the crystals by phagocytosis in a process that induced disruption of cell–cell adhesion, release of reactive oxygen species and membrane damage, events that may be linked to the release of inflammatory cytokines by these cells into the culture media. In conclusion, calcium oxalate crystals found in commercially available FBS are toxic to cells, and their presence may confound results from in vitro studies where, amongst others, phagocytosis, biomineralization, renal cell and molecular biology, and drug and biomaterial testing are being examined. J. Cell. Biochem. 103: 1379–1393, 2008.

Key words: fetal bovine serum; calcium oxalate; cell culture; biomineralization; phagocytosis

Cell culture methods and models are in widespread use and they are often central to many (if not most) life science investigations. Fetal bovine serum (FBS) is commonly used in cell and molecular biology studies as an additive whose constituents promote cell survival, proliferation and differentiation. Commercially available FBS is only partly characterized, and despite ultra-filtration steps used by the suppliers, the presence of particulate material found in such products when delivered to laboratories worldwide apparently has been either intentionally disregarded as being trivial, or overlooked. A novel observation reported here is that we routinely observed inorganic, mineral crystals (calcium oxalate) in practically all lots of FBS obtained from different suppliers. Crystals were first observed as particulate material in cell cultures grown in Dulbecco's Modified Eagle's Medium (DMEM) supplemented with 10% FBS, without filtering. Further examination by light microscopy of the medium and the serum separately identified the latter as the source of crystalline material. FBS is currently delivered by its suppliers with a list of quality-assurance standards that include validated mycoplasma removal, ultra-low endotoxin and hemoglobin levels, sequential filtration through a 100-nm filter followed by a 40-nm filter, lot-to-lot consistency checks and other quality control tests. FBS has a complex composition that includes salts of calcium, potassium, phosphate and sodium, and other constituents such as cholesterol, cortisol, parathyroid hormone, prolactin, and prostaglandins E and F, glucose, hemoglobin, uric acid, creatine, alkaline phosphatase, albumin and insulin; total protein can average 3.8 g/100 ml [Staines and Price, 2003].

*Correspondence to: Marc D. McKee, Faculty of Dentistry, McGill University, 3640 University Street, Montreal, Quebec, Canada H3A 2B2. E-mail: marc.mckee@mcgill.ca

Received 26 April 2007; Accepted 5 July 2007

DOI 10.1002/jcb.21515

Calcium oxalate (CaOx) is one of the major mineral phases commonly found in human kidney stones where it exists mainly in its monohydrate (triclinic) form; in urine, its dihydrate (tetragonal) state is also common, and both crystalline forms have been found in urine of patients suffering from kidney stones and in urine of normal subjects [Elliot and Rabinowitz, 1980]. Calcium oxalate monohydrate (COM) crystals found in urine may be spindle-, oval-, tabular- or dumbbell-shaped, and vary considerably in size [Burns and Finlayson, 1980; Akbarieh et al., 1987]. Calcium oxalate dihydrate (COD) crystals in urine are tetragonal, di-pyramidal minerals that also vary in size but typically have dimensions in the micrometer range. While other mineral phases can exist in urine, composite mineral phases having variable appearances may result from epitaxial growth of one mineral phase on another; however, in our study of FBS, mainly COD was observed, with minor amounts of COM and even lesser amounts of unidentified particulates.

In organismal systems and tissues that undergo biomineralization, whether physiologic or pathologic, the crystalline mineral phase is invariably associated with either an abundant organic extracellular matrix, or a limited or diverse array of specific, mineral-binding proteins that reside at the mineral surface and are occluded within [Ryall, 2004]. In circulating plasma (from which commercial serum [FBS] is derived), mineral ion-binding proteins are also common, some of which (α_2HS-glycoprotein [also known as fetuin-A] and matrix Gla protein) are thought to stabilize critical mineral nuclei to prevent their precipitation as larger crystals in the circulation [Schafer et al., 2003; Price et al., 2004]. More specifically, bovine fetuin-A purified from serum is a potent inhibitor of the precipitation of calcium-phosphate mineral phases from supersaturated solutions of calcium phosphate [Schinke et al., 1996]. Amongst many proteins known to regulate different types of mineralization in diverse systems, osteopontin, Tamm-Horsfall protein, nephrocalcin, calprotextin, human serum albumin, and prothrombin fragments are proteins known to modulate CaOx and calcium-phosphate crystal growth, and these proteins represent the major organic phase present in most kidney stones [El-Shall et al., 2004]. Exposure of renal epithelial cells in culture to both oxalate and CaOx crystals induces an early form of cell injury associated with the production of free radicals (superoxide and hydroxyl radicals), lipid peroxidation and release of lactate dehydrogenase (LDH) [Thamilselvan et al., 2000].

In this manuscript, we provide a detailed analysis of the calcium oxalate mineral phase found in various lots of FBS from different major commercial suppliers, and describe the binding of proteins to this mineral. The significance of this finding to the scientific community at large who employ cell culture methods is that these crystals may sequester mineral-binding proteins (e.g., essential growth factors) and ions that affect, amongst other processes, cell metabolism, signaling, adhesion, proliferation and migration. The presence, number and size (and thus the surface area available for adsorption of organic constituents) of these crystals, may determine the activity of the FBS essential for observing selected biological activities in vitro. Indeed, it is common practice amongst investigators to screen lots of serum, prior to full-scale use, for their efficacy in eliciting a desired biological response from the cells of interest—differences in activity we feel can be at least partly ascribed to the presence of CaOx crystals in FBS. More specifically, our manuscript presents data on specific effects of the presence of such crystals in terms of cell toxicity and in terms of their effects on cell culture studies of phagocytosis. In the latter case, CaOx crystals themselves can be phagocytosed by the cells under investigation, thus potentially confounding experimental results where the phagocytosis of other particulates or infectious organisms of interest (e.g., bacteria, leishmania) are being studied. Our observations are also pertinent to biomineralization studies in vitro where similar concentrations of FBS are used [Franceschi and Iyer, 1992; Marsh et al., 1995] and where mineral-binding/regulating proteins might be sequestered by the CaOx crystals, and to biomaterial and drug-testing studies.

METHODS

Cell Culture

To investigate the source and nature of the crystals observed by light microscopy in FBS, and in cell cultures after addition of FBS, samples of FBS were purchased from four major suppliers of bovine serum in North America;

namely, Invitrogen (Gibco), HyClone, Clontech and Wisent Laboratories. Sera were stored frozen at −20°C and thawed as recommended by the supplier. In brief, frozen serum was thawed in a 37°C water bath with gentle shaking every 15 min. In total, 27 different bottles of FBS from the four suppliers and corresponding to 19 different lots of serum were screened for the presence of crystalline material. Buffer preparation and washing of crystals were done with HPLC-grade water (Millipore-Simplicity system). OPN antibody against bovine bone OPN was a gift from Dr. E. Salih (Harvard University, Children's Hospital Medical Center, Boston); sheep anti-bovine fetuin-A was a gift from Dr. W. Jahnen-Dechent (University of Aachen, Germany); goat anti-mouse and goat anti-sheep secondary antibodies were purchased from Amersham Biosciences. Calcium oxalate monohydrate (COM) was purchased from Sigma–Aldrich, and calcium oxalate dihydrate (COD) crystals were synthesized as described by Lepage and Tawashi [1982]. Briefly, for the synthesis of COD, 3 ml of 0.005 M sodium oxalate solution were added to 5 ml of 1 M calcium chloride solution, drop-by-drop, using a pipette. The mixture was left without agitation for 24 h at 4°C, and the crystals were harvested by centrifugation at 6,000*g* for 5 min. Full-length, phosphorylated bovine milk osteopontin was from Arla Foods (Denmark) prepared according to methods similar to those developed by Sorensen and Petersen [1993]. J774A.1 macrophage-like cells purchased from American Type Culture Collection (ATCC) were grown in Dulbecco's Modified Eagle's Medium (DMEM) with 10% FBS, 4 mM L-Glu, 1.5 g/l sodium bicarbonate and 4.5 g/l glucose. NIH/3T3 fibroblasts were purchased from ATCC and were grown in low-bicarbonate DMEM supplemented with either 10% FBS or 10% bovine calf serum (BCS). Oregon Green-488 phalloidin® and Live/Dead® viability/cytotoxicity kit (Calcein AM and ethidium homodimer-1) were purchased from Invitrogen (Molecular Probes). Gene Ruler™ 100 bp DNA ladder plus was from Fermentas.

Microscopic Examination, Scanning Electron Microscopy and X-Ray Microanalysis, Atomic Force Microscopy, and X-Ray Diffraction Analysis of Crystals Harvested From FBS

Routine harvesting of crystals from FBS was done by centrifugation using an IEC Multi RF (Thermo IEC) centrifuge; examination of FBS aliquots (with crystals) was done by light microscopy. Fifteen- or 50-ml aliquots were centrifuged at 9,000*g* for 15 min at 15°C followed by washing of the crystals with HPLC-grade water. The crystals were examined by light microscopy at magnifications of 100–400×. Large-scale collection of CaOx crystals was performed as described above, followed by extensive washing with 0.1 M sodium hydroxide and/or 10 mM Tris buffer to remove contaminating material. For scanning electron microscopy (SEM), 20 μl of crystal suspension was dried at room temperature and mounted on metallic stubs. The samples were sputter-coated (20 nm) with Au and Pd for 2 min and examined using a FEG-SEM Hitachi S-4700 microscope. Energy-dispersive X-ray microanalysis was performed using an Oxford INCA microanalysis system (Model D-7200) with its installed software INCA Microanalysis Suite (Version 4.04). For powder X-ray diffraction analysis, the crystalline material was collected as described above, and the crystals were resuspended in absolute ethanol and pipetted onto a glass coverslip and analyzed as described previously [Thrall et al., 1985]. Briefly, X-ray diffraction analysis was performed with Cu Kα X-rays on a Philips powder X-ray diffractometer (Model PW 1710). The diffraction spectra were acquired by X'Pert Quantify (Version 1.0) software and processed by X'Pert High Score (Version 2.0) software with reference to Powder Diffraction File database (Version 4+ 2005) of the International Centre for Diffraction Data (Newton Square, PA).

For imaging of crystals by atomic force microscopy (AFM), the crystalline material harvested from FBS was immobilized onto a self-assembled monolayer (SAM) substrate; the SAM substrates were prepared according to Finklea and Hanshew [1992]. Briefly, commercially available gold substrates (Evaporated Metal Films, Inc.) were immersed into dilute thiol-ethanol solutions (11-mercaptoundecanoic acid, 95%, ~1.0 mM) for 24–36 h. Crystals dispersed in 20 μl of ethyl alcohol were transferred onto freshly prepared SAM substrates and incubated for 10 min to allow the crystals to settle onto the substrate. Surfaces with crystals were gently dried with a stream of pure, dry nitrogen gas, and were immediately imaged by AFM in air using a Multimode Nanoscope IIIa Scanning Probe Microscope (Digital

Instruments) operating in the tapping mode, with a piezoelectric scanner capable of x- and y-scan range at 125 μm. Height and phase AFM images were collected, processed (flattening and x–y order planefit) and analyzed (section and zooming) using the Nanoscope IIIa Digital software (Version 5.30r3sr3).

Computer Modeling and Software Identification of Crystallographic Faces

The morphologies of CaOx crystals collected from FBS were identified and indexed by comparing an observed morphology with its angle of polar-type corners of faces (i.e., crystal corners intersecting the *c*-axis of CaOx) to graphic renditions prepared by the computer software SHAPE (Version 6.0, 2000, E. Dowty, Kingsport, TN; www.shapesoftware.com), with reference to unit cell parameters and X-ray powder diffraction file data for CaOx.

SDS–PAGE and Western Blotting of CaOx Crystal-Associated Proteins

Crystals were collected from 500 ml of FBS as described above and protein analysis was performed by SDS–PAGE and Western blotting. To release crystal-bound proteins, pellets of crystals were boiled for 5 min with 50 μl of 2× protein-loading buffer containing 10% SDS and 2.5 mM 2-mercaptoethanol. Following electrophoresis, the gels were stained with silver nitrate or used for Western blotting. For silver staining, the gels were fixed with ethanol–acetic acid, sensitized with sodium thiosulfate and stained with silver nitrate. The gels were then scanned or photographed.

DNA Binding to CaOx Crystals

Synthetic COM or COD crystals, at a concentration of 200 μg/ml, were incubated first in DMEM medium for 2 h at room temperature followed by incubation for 2 h with plasmid DNA (pDNA; gWiz, Aldevron, CA) at a concentration of 10 μg/ml pDNA. Crystals were washed with 10 mM Tris buffer (pH 7.6) to remove unbound pDNA, and harvested by centrifugation. The pellet of crystals with bound pDNA was resuspended in 40 μl of loading buffer and loaded into the wells of a 0.8% agarose-ethidium bromide gel. After electrophoresis, the gels were photographed using a Bio-Rad Gel-Chemi doc system.

Oxalate and Calcium Measurements

Oxalate determination was done using an enzymatic method (Trinity Biotech) based on the oxidation of oxalate followed by measurement of hydrogen peroxide produced during the reaction by a peroxidase-catalyzed reaction [Chiriboga, 1963]. In brief, crystals harvested from FBS were acid-boiled to solubilize any oxalate crystals present in the sample, and then they were treated with ascorbate oxidase (Sigma) and then TCA (trichloroacetic acid) for removing and precipitating potentially interfering substances. The pH of the samples was adjusted followed by activated charcoal incubation, centrifugation and filtration steps. Oxalate standards provided with the kit were prepared, and the concentration of oxalate in the processed FBS crystal samples was calculated using absorbances obtained from standard, control measurements. Readings were done at 590 nm using a microplate reader (Model EL800, Bio-Instruments, Inc.). A calcium assay kit (Diagnostic Chemicals Ltd) based on Arsenazo III dye coupling was used to determine the calcium concentration of crystals harvested from FBS. Crystals were solubilized in 2 N HCl and aliquots of deionized water, the standard and the samples to be assayed were added to separate plastic tubes. One ml of reagent was added, followed by incubation for 15 min at room temperature. The absorbance was determined at 650 nm using a Fluostar Optima (BMG Labtech) reader.

Solubility of COD Crystals Under Cell Culture Conditions

FBS (containing $\sim 6 \times 10^5$ crystals/l) was prepared as a 10% solution in DMEM as is commonly used in most in vitro studies and as was used in our culture experiments with cells. One hundred microliters of this DMEM-diluted FBS was aliquoted (in quadruplicates) into 96-well culture plates. After incubation at 37°C and 5% CO_2 for 24 h, wells were examined independently by light microscopy for the presence of crystals. Birefringent di-pyramidal crystals were counted and representative images were recorded. These experiments were done in the absence of cells since their presence makes it difficult to differentiate crystals from cellular background elements and thus to provide accurate counts.

Phagocytosis of CaOx Crystals by Macrophages, and Actin Staining

J774A.1 and NIH/3T3 cells were plated at a density of 15,000 cells/cm^2 and incubated for 48 h followed by washing with DMEM. After addition of 200 μg/ml of COM or COD to the cells, the plates were incubated at 37°C with 5% CO_2 for 16 h. Some of the wells were treated with LysoTracker® Red DND-99 (Invitrogen–Molecular Probes) to stain phagolysosomes. To stain F-actin, the culture dishes were fixed with paraformaldehyde, washed with phosphate buffered saline (PBS) and then incubated with Oregon Green-phalloidin. Samples were viewed by immunofluorescence microscopy and pictures were taken with Leica DC 300F camera mounted on a phase contrast/fluorescence microscope (Leica DM IL).

Determination of Cell Membrane Integrity and Reactive Oxygen Species (ROS)

Cell membrane integrity was evaluated using a Live/Dead® Viability/Cytotoxicity assay kit. Calcein AM does not fluoresce until it is transformed into an intensively green fluorescing calcein by nonspecific cytoplasmic esterase. After exposure of J774A.1 cells to CaOx, the fluorescent probes were added and the cells incubated at 37°C for different lengths of time; the resulting changes induced by CaOx were assessed by fluorescence microscopy.

Amino phenyl fluorescein (APF) was used as an indicator of reactive oxygen species (ROS). APF is nonfluorescent until it reacts with the hydroxyl (OH) radical, peroxynitrite anion or hypochlorite anion ($^-$OCl). J774A.1 cells plated at a density of 15,000 cells/cm^2 were washed with PBS to remove interfering bovine serum albumin (BSA) or phenol red from the culture medium. Cells were then incubated with APF followed by incubation with COD crystals or H_2O_2 at 37°C and 5% CO_2. Intracellular fluorescence was measured using excitation/emission wavelengths of 490/515 nm, and microscopic images were recorded.

Cell Proliferation

Since proliferating cells are metabolically more active than non-proliferating cells, we used the tetrazolium assay to measure cell proliferation. Two hundred microliters of cell suspension containing 1×10^4 cells was added to a 96-well plate. After culturing for 24 h, the cells were treated with CaOx crystals and incubated for different times at which point the medium was replaced with medium containing 0.25 mg/ml of MTT (3-(4,5-dimethylthiazol-2-yl)-2,5-diphenyltetrazolium bromide). The cells were incubated for an additional 3 h and the precipitated reaction product (formazan crystals) was dissolved with 200 μl of DMSO. Absorbance values were determined with a microplate reader using a 550 nm filter.

RESULTS

Characterization of CaOx Crystals Collected From FBS

Inspection by light microscopy of aliquots collected from different lots and bottles of FBS obtained from different suppliers revealed the presence of tetragonal, di-pyramidal, optically transparent crystals varying in size, shape and number (Fig. 1A). Scanning electron microscopy of the isolated crystals revealed morphologies with distinct crystallographic faces (Fig. 1B) characteristic of COD, and occasionally other crystals having different morphologies (Fig. 1B, inset). Determination of elemental composition by energy-dispersive X-ray microanalysis (Fig. 1C) of the crystals revealed the presence of calcium, carbon and oxygen—an elemental signature characteristic of CaOx. The same analyses performed on COD crystals prepared synthetically in our laboratory (Fig. 1D–F) validated our identification of COD crystals in FBS.

X-ray diffraction analysis of the CaOx crystals collected from FBS revealed diffraction maxima (spectral peaks) consistent with a mixture of monohydrate (Whewellite) and dihydrate (Weddellite) phases (Fig. 2A–C). Individual di-pyramidal crystals were further confirmed as being the dihydrate phase of CaOx by imaging and quantitative height measurement using tapping-mode AFM. The dominant face of COD from FBS develops from a single, triangular spiral growth hillock, and evidence for protein binding was observed as particulate material on the flat terraces of the crystals (Fig. 2D), although this could also be inorganic material. The growth hillock contains a COD-characteristic polar angle of 76°, and its shape can be related to the symmetry of the {1 0 1} faces of COD using SHAPE software for identification of crystallographic faces (Fig. 2E). By AFM, individual crystal growth steps were

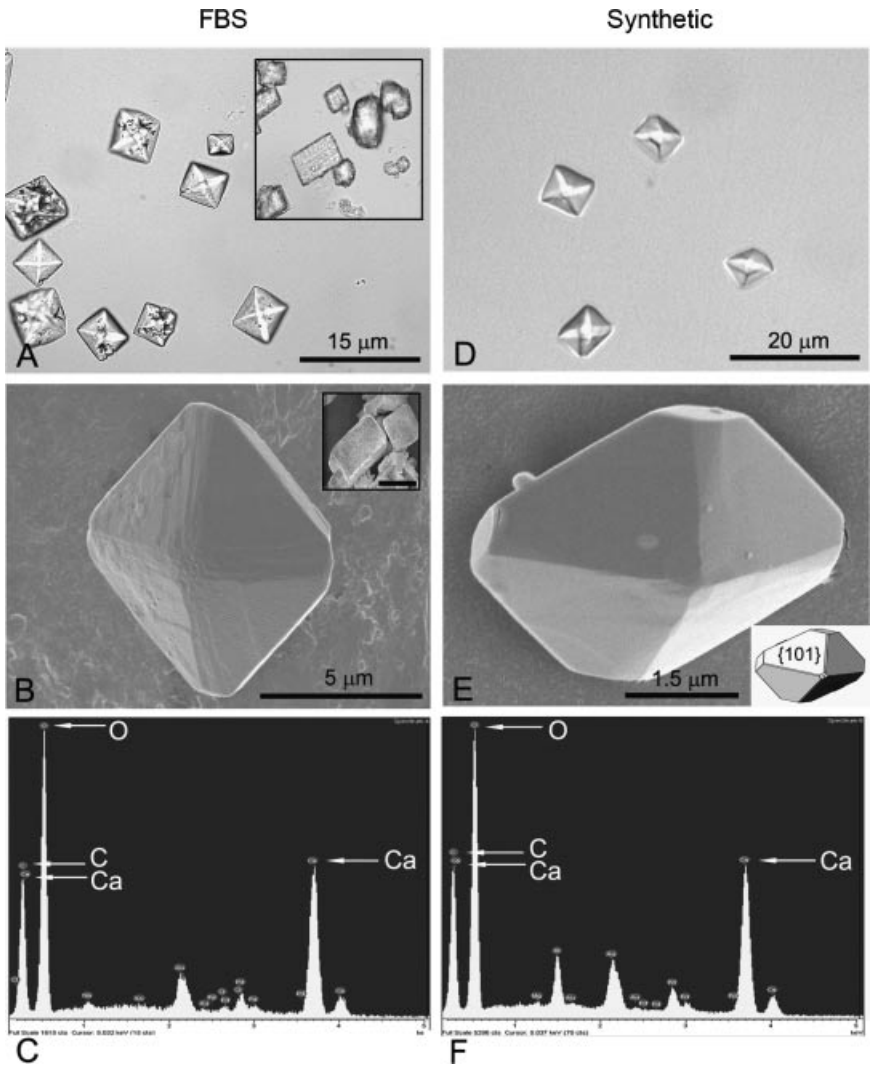

Fig. 1. Micrographs of crystals harvested from commercially available FBS, and synthetic CaOx crystals. **A**: Light micrograph of the most common crystal type found in FBS (inset shows additional crystal morphologies occasionally observed). **B**: SEM micrograph of crystals harvested from FBS showing di-pyramidal shape characteristic of COD crystals (inset shows additional crystal morphologies occasionally observed). **C**: EDX microanalysis of crystals harvested from FBS. Major spectral peaks correspond to calcium (Ca) carbon (C) and oxygen (O), their presence and magnitude (counts) being consistent with the elemental composition of CaOx. **D**: Light micrograph of synthetic COD crystals. **E**: SEM micrograph of synthetic COD crystals showing di-pyramidal morphology characteristic of COD (inset shows corresponding SHAPE software schematic identifying the dominant {1 0 1} crystallographic faces). **F**: EDX microanalysis of synthetic COD crystals showing characteristic COD major spectral peaks for Ca, O and C.

approximately 6.30 (±0.03) nm in height (Fig. 2F,G), here corresponding to a macrostep of 10 monomolecular layers of COD (a monostep has a height of 0.63 nm, the *d*-spacing of COD {1 0 1} faces). Analyses of other similar crystals routinely showed macrostep heights as a multiple of the monolayer height, confirming this face characterization of COD. The formation of {1 0 1} faces by the spiral growth mechanism (vs. the birth-and-spread growth mechanism) suggested that these CaOx crystals grew (or dissolved) in an orderly, relatively slow surface-controlled fashion on these faces [Lasaga, 1998], likely also involving protein-mineral. Consequently, in FBS, both calcium levels and selected proteins that bind to these {1 0 1} faces are constantly and effectively locally scavenged by the controlled growth (or release by dissolution) of these crystals, and likely do not occur as a result of rapid and uncontrolled phase changes during handling of the FBS.

Crystal counts were obtained using a Neubauer chamber slide, providing values that ranged from 13.2×10^5 to 10×10^6 crystals per

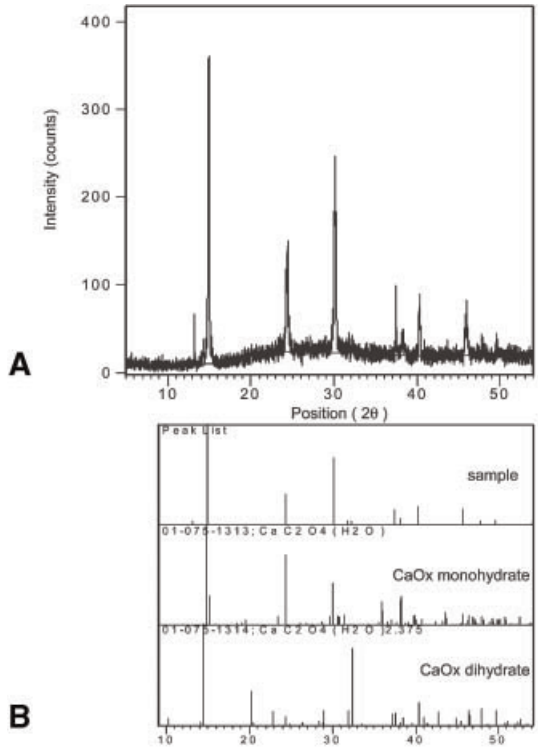

Position (degree,2θ)	d-spacing (angstrom)	Matched by (PDF)
14.9235	5.93646	01-075-1313
24.3427	3.65657	01-075-1313, 01-075-1314
30.1190	2.96717	01-075-1313
31.8053	2.81360	01-075-1314
32.2263	2.77780	01-075-1313, 01-075-1314
37.4230	2.40315	01-075-1313, 01-075-1314
38.1868	2.35682	01-075-1313, 01-075-1314
40.2586	2.24018	01-075-1313, 01-075-1314
45.8343	1.97981	01-075-1313, 01-075-1314
47.9377	1.89774	01-075-1313, 01-075-1314
49.6151	1.83744	01-075-1313, 01-075-1314
54.1664	1.69331	01-075-1313, 01-075-1314

C 01-075-1313: Whewellite, calcium oxalate monohydrate, $CaC_2O_4(H_2O)$
01-075-1314: Weddellite, calcium oxalate dihydrate, $CaC_2O_4(H_2O)_2$

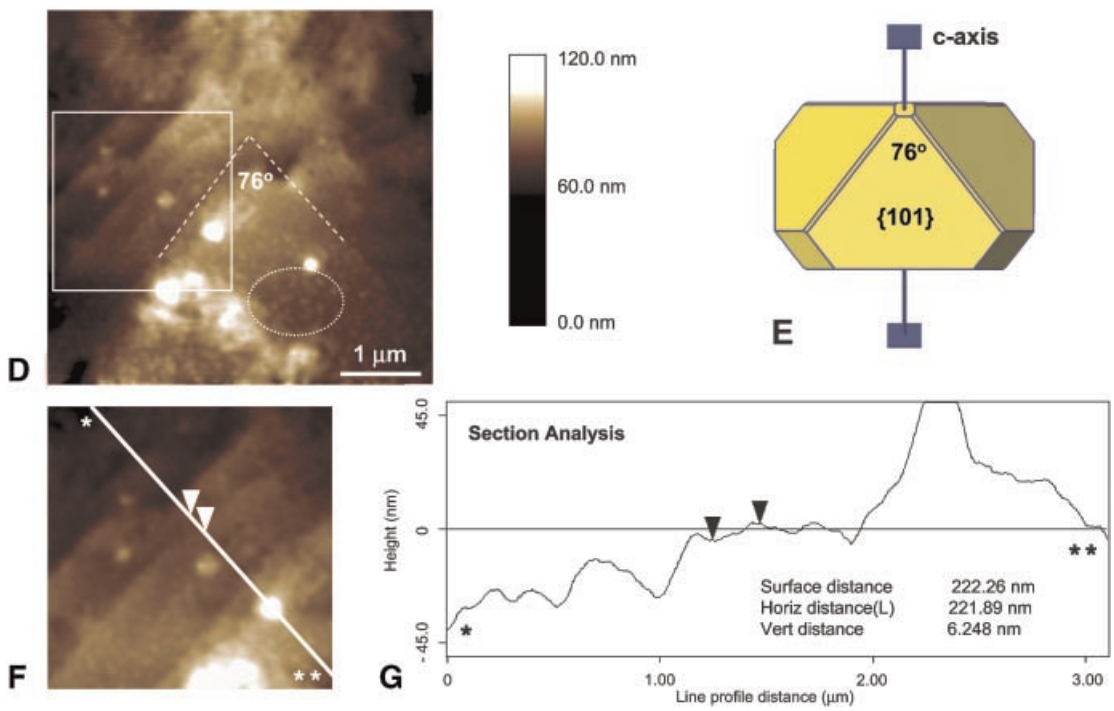

Fig. 2. **A**: X-ray diffraction spectrum obtained from CaOx crystals harvested from FBS. **B**: Comparison of the identified 2θ spectral peaks in the FBS CaOx with COD and COM standards indicate a mixture of both monohydrate and dihydrate phases in the sample. **C**: Tabular listing of the details of the identified major Kα (2θ) peaks showing atomic lattice *d*-spacings as matched with the standard powder diffraction files (PDF) of the International Centre for Diffraction Data. **D:** AFM height image showing a {1 0 1} face of a COD crystal harvested from FBS that formed via a single spiral growth hillock. A polar corner of 76° exists on the flat terrace, indicating the crystallographic orientation of the growth hillock (see also graphic rendition in **E**). The oval inset (in D) indicates a possible region of globular proteins adsorbed onto the flat terrace of the {1 0 1} face. E: SHAPE software graphic rendition of the COD crystal imaged in D showing overall crystal morphology and *c*-axis orientation of the analyzed crystal. **F**,**G**: Section analysis by AFM (enlargement of white boxed area in D) showing that a measured crystal growth step height (vertical distance between the arrowheads) of adjacent steps (6.248 nm) is essentially an integral multiple of the 0.632 nm *d*-spacing characteristic of the {1 0 1} face for COD. [Color figure can be viewed in the online issue, which is available at www.interscience.wiley.com.]

liter of FBS. Oxalate concentrations in FBS were estimated using a modified clinical protocol and they ranged from 0.030 to 0.060 mmol/l in three bottles of FBS examined from different suppliers. Oxalate values in human urine as described by the manufacturer of the oxalate kit range from 0.1 to 1.2 mmol/l. The calcium content of crystals harvested from FBS varied from 0.1 to 1.0 mmol/l. CaOx crystals were also observed in heat-inactivated FBS and BCS.

Silver Staining and Western Blotting of CaOx Crystal-Associated Proteins

Given that proteins are well-known modulators of crystal nucleation and growth, we decided to investigate whether bovine serum proteins were associated with the CaOx crystals harvested from FBS. After extraction of mineral-bound proteins from the FBS crystals and SDS–PAGE, staining with silver nitrate revealed a large number of protein bands ranging in molecular weight from less than 25 kDa to more than 150 kDa (Fig. 3A, lanes FBS1-3). This association was further confirmed by incubation of synthetic COM and COD crystals with FBS (devoid of crystals, removed by centrifugation). Silver staining of proteins similarly eluted from the synthetic crystals (Fig. 3A, lanes COM and COD) likewise showed numerous protein bands with broadly ranging molecular weights. Whereas protein binding to crystals varied considerably amongst different lots of FBS from different suppliers, the protein-binding profiles from FBS were similar for both COM and COD.

Based on the abundant literature describing OPN and fetuin-A as mineral-binding proteins, and as potent circulating (plasma) inhibitors of calcification, immunoblotting was used to investigate whether these proteins were bound to the crystals isolated from FBS and to the synthetic crystals incubated with FBS. Figure 3B shows Western blots of protein bands reacting with antibodies against OPN (42–80 kDa) or fetuin-A (59 kDa). OPN was identified amongst proteins eluted from crystals harvested from FBS as well as from synthetic crystals incubated with FBS. The appearance of OPN bands having different molecular weights as shown in Fig. 3B is common, and has been reported previously [Bautista et al., 1996]. CaOx crystals from some lots of FBS show fetuin-A binding as revealed by Western blotting (Fig. 3B). Collectively, these results are consistent with previous reports showing the association of OPN with CaOx crystals [Konya et al., 2003] and the presence of fetuin in a protein-mineral complex in serum [Price et al., 2002].

Since DNA binds to calcium-phosphate minerals [Olton et al., 2007], we investigated whether plasmid DNA was able to bind to CaOx crystals. Figure 3C shows DNA released from crystals as visualized using agarose gel electrophoresis; the affinity of plasmid DNA for the

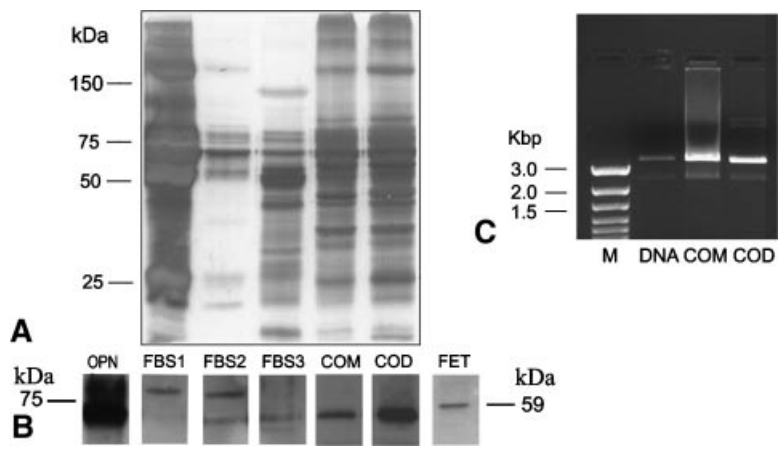

Fig. 3. Binding of macromolecules to CaOx. **A**: PAGE-separated, and silver-stained, proteins eluted from CaOx crystals collected from three different lots from different suppliers of FBS (lanes FBS1–3), and from synthetic COM and COD crystals incubated with FBS (lanes COM and COD). **B**: Western blots for OPN (anti-bovine OPN) of proteins eluted from CaOx crystals collected from different lots of FBS (lanes FBS1–3), and from synthetic COM and COD crystals incubated with FBS (lanes COM and COD). The first lane at the left (OPN) corresponds to a Western blot of purified OPN. CaOx crystals from some lots of FBS show fetuin-A binding as revealed by Western blotting using anti-bovine fetuin-A (last lane at the right, FET). **C**: Agarose gel electrophoresis of adsorbed plasmid DNA (lane DNA) eluted from synthetic COM and COD crystals (lanes COM and COD, respectively). Lane M = 100 bp DNA ladder markers. DNA = 5.7 kbp plasmid DNA.

monohydrate form (COM) of CaOx seems to be higher than the affinity for the dihydrate (COD) form.

Solubility of COD Under Cell Culture Conditions

Since the characterization of the COD mineral was performed on crystals collected directly from undiluted FBS, we then examined the solubility of the crystals under standard cell culture conditions where FBS is typically diluted 10-fold with DMEM (i.e., 10% FBS). Under these conditions (without cells), over an incubation period of 24 h at 37°C, COD crystals slowly dissolved (Fig. 4). Crystals decreased in number with time, and slowly lost their di-pyramidal morphology such that by 24 h, crystals were essentially absent from the diluted FBS. Belliveau and Griffin [2001] studied the solubility of CaOx in cell culture media and reported equilibrium parameters for CaOx in DMEM and McCoys 5A medium), but such data is not available for medium supplemented with FBS.

Phagocytosis of CaOx by Macrophages and Mouse Fibroblasts

In vivo, insoluble particulates are typically cleared in tissues and in the circulation by macrophages via phagocytosis. To model this in vitro, we used the J774A.1 macrophage cell line to study the fate of CaOx crystals when added to cultures of these cells. For comparison, NIH/3T3 mouse fibroblasts were also used to investigate phagocytosis of the crystals, since most cell types are capable of at least some degree of phagocytosis. In both cases, binding of crystals to cells occurred rapidly (within a few minutes of exposure), and the crystals soon became internalized within the cells. After 12–24 h, the cytoplasm of the cells appeared variably loaded with crystals (Fig. 5). Internalization of the crystals was confirmed by extensive washing and by incubating the cells with LysoTracker™, a probe for labeling and tracing lysosomes and phagolysosomes in living cells (Fig. 5, top inset in upper-right panel). Phagocytosis of CaOx was also confirmed in stimulated primary mouse macrophages obtained by peritoneal lavage (data not shown).

Actin Staining, ROS Production and Membrane Damage in Cells Exposed to CaOx

While no substantive changes were observed in the actin cytoskeleton after addition of CaOx crystals to the cell lines used in this study (data not shown), phagocytosis is nevertheless known to occur via an actin-dependent mechanism [Aderem and Underhill, 1999] resulting in other cellular and metabolic changes. Addition of COD crystals to J774A.1 macrophages resulted in internalization of the crystals (Fig. 6A) and a significant loss of intercellular contact and cell adhesion.

Animal models as well as tissue culture studies indicate that exposure to high levels of oxalate and CaOx crystals is injurious to cells [Khan, 2004]. Mammalian cells are known to produce free radicals when exposed to CaOx crystals [Umekawa et al., 2003], and previous studies have shown that macrophages produce superoxide anion (O_2^-) as well as nitric oxide

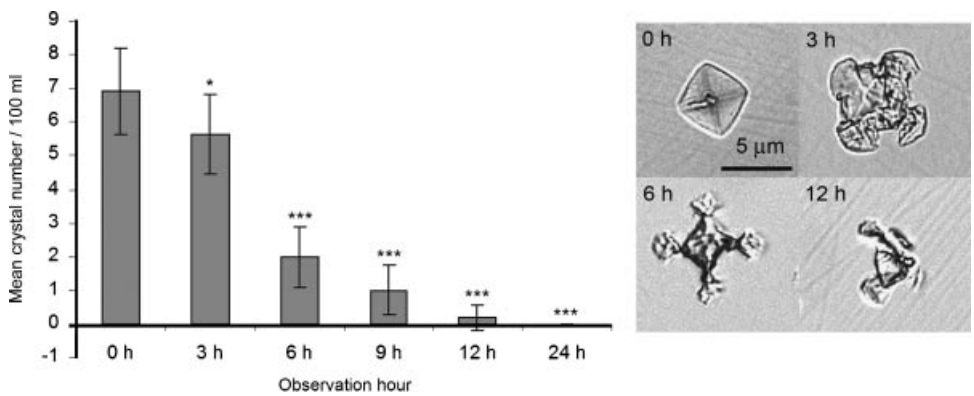

Fig. 4. Quantification of crystal numbers in FBS diluted 10-fold with DMEM (i.e., 10% FBS) over a 24 h incubation period at 5% CO_2 and 37°C. CaOx crystal counts decreased with time such that crystals were essentially absent after 24 h of incubation (**left panel**). Progressive dissolution of the CaOx was associated with changes in morphology from the original di-pyramidal shape of the crystals (**right panel**). $^*P < 0.05$ and $^{***}P < 0.0001$ as compared to counts at the start of the incubation (0 h). Data are reported as mean ± standard error of mean and from triplicate analyses.

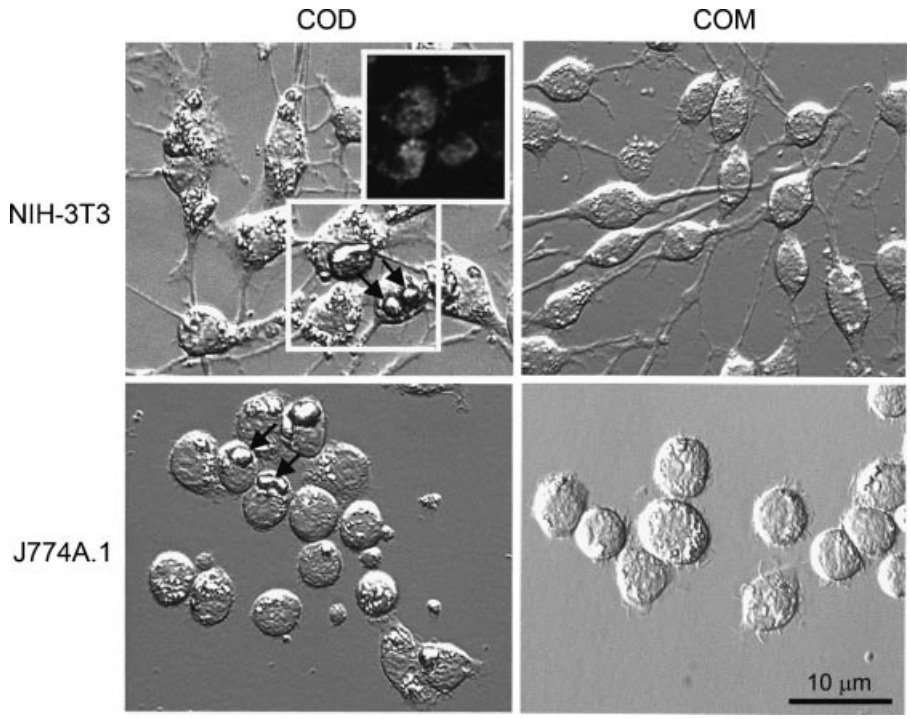

Fig. 5. Phagocytosis of COD and COM crystals by NIH/3T3 fibroblasts and J774A.1 macrophages. Light micrographs show internalized crystals (arrows) in both cell types after a 16-h exposure to COD and COM crystals. The matching insets in the upper left panel show a region stained by LysoTracker™; red fluorescent areas indicate a high concentration of punctate phagolysosomes in close proximity to the internalized crystals.

(NO) [Hassoun and Wang, 1999]. ROS generation was evaluated in J774A.1 cells treated with CaOx crystals using APF as a probe for ROS. Figure 6B shows generation of ROS by cells exposed to COD crystals as compared to the known high production of ROS following exposure to hydrogen peroxide (Fig. 6C).

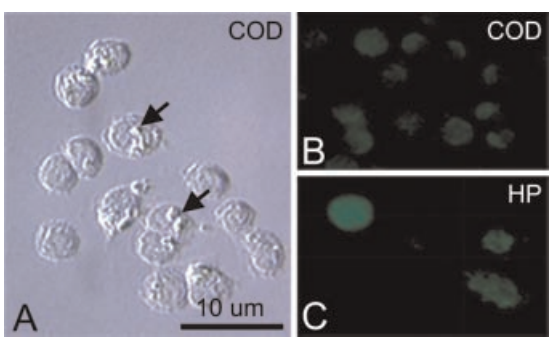

Fig. 6. **A**: Light micrograph of cells exposed to COD crystals. Granular regions in the cytoplasm indicate the presence of internalized crystals (arrows). Starting from an initially confluent monolayer of J774A.1, cells have lost cell–cell contact and adherence, indicating an effect of phagocytosis on these cell activities. **B**: ROS induction and detection (with APF) of cells exposed to 200 μg of COD crystals (**C**) and 100 μM hydrogen peroxide (H_2O_2; HP) as control. Green fluorescence indicates a reaction between APF and hydroxyl radical, hypochlorite anion or peroxynitrite anion.

Calcein AM and ethidium homodimer-1 are commonly used to study membrane integrity and degree of apoptosis [Bratosin et al., 2005]. Here, we used these staining reagents to investigate toxic effects of CaOx crystals on J774A.1 macrophages. Without addition of CaOx crystals, cells exposed to both reagents showed calcein AM uptake and retention in the cells, and no staining of nuclear DNA by ethidium homodimer-1 (Fig. 7A,B). In contrast, cells treated similarly but also with the addition of CaOx crystals showed nuclear staining by ethidium homodimer-1 and leaking of calcein AM attributable to membrane damage (Fig. 7C,D). These results are in agreement with previous studies showing induction of ROS and membrane damage after exposure of mammalian cells (renal epithelial cells) to CaOx [Greene et al., 2005].

Effect of CaOx on Cell Proliferation

CaOx crystals readily attached to the surface of the cells, and phagocytosis occurred within a few minutes after exposure to the crystals. To investigate potential effects on cell proliferation, sub-confluent cultures of NIH/3T3

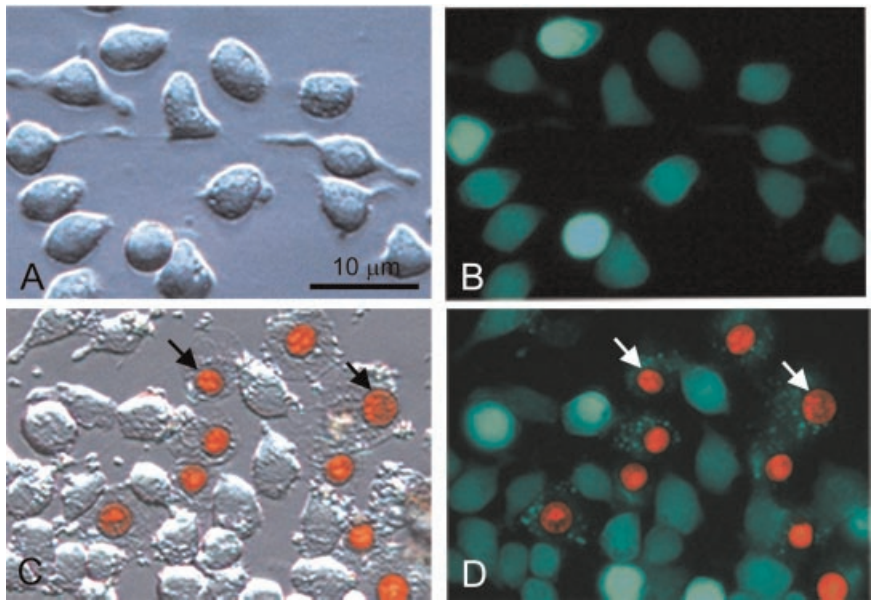

Fig. 7. Membrane integrity of J774A.1 macrophages exposed to COD and stained with calcein AM and ethidium homodimer-1. **A**: Photomicrograph of control cells (without added COD) displaying normal morphology. **B**: Micrograph of the same cells shown in panel A after staining with calcein AM and ethidium homodimer-1. Plasma membrane-intact cells retain calcein (green fluorescence) and nuclei do not stain with ethidium homodimer-1. **C**: Micrograph of cells exposed to COD crystals showing nuclear red fluorescence from staining with ethidium homodimer-1 (arrows) in plasma membrane-damaged cells. **D**: Merge of panels C and D to show loss of calcein AM staining, and gain of ethidium homodimer-1 staining, in the same cells (arrows) after plasma membrane damage following exposure to COD crystals.

fibroblasts were exposed to the crystals and were further incubated for 6–24 h and cell proliferation was assessed by reduction of the tetrazolium salt (MTT). COM and COD crystals stimulated MTT reduction in a time-dependent manner (Fig. 8). Reduction of MTT was statistically significant at 6 and 12 h after both COD and COM crystal exposure. After 24 h, the values of CaOx-treated cells reached proliferation values similar to cells without addition of CaOx.

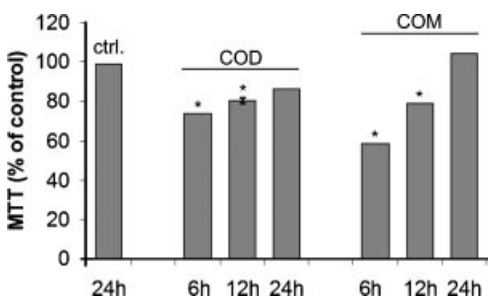

Fig. 8. Proliferation of NIH/3T3 fibroblasts (using the MTT assay) after exposure to CaOx crystals. Cells were exposed to 200 μg/ml of either COD or COM crystals for the indicated time. Results are presented as a percentage of cell proliferation relative to control. While inhibiting cell proliferation at 6 and 12 h ($P < 0.05$) after CaOx crystal exposure, at 24 h, cell proliferation returned to values similar to those of control cells (without added CaOx crystals). Data are reported as mean ± standard deviation and from triplicate analyses.

DISCUSSION

We report here the novel observation that commercial FBS from several major suppliers consistently contains abundant inorganic mineral crystals, and provide a detailed characterization of these crystals as predominantly calcium oxalate dihydrate (COD, Weddellite). Moreover, we have determined that the crystals bind and sequester mineralization-regulating serum proteins from the FBS, and that they also have the potential to bind DNA. Finally, we report that exposure of mammalian cells in culture to these crystals induces their internalization by phagocytosis, and that cytotoxic and proliferation effects are a consequence of this exposure. Such observations indicate that caution is warranted when using FBS as a cell- and tissue-culture additive for in vitro studies on phagocytosis, biomineralization, and biomaterial and drug testing.

Despite the widespread use of FBS as a basal medium supplement in mammalian cell and tissue culture protocols, little attention has been given to the variable composition of bovine

serum—a by-product of the beef-packing industry. Unless critical to experimental design and outcomes, few investigators take the time and effort to characterize the FBS they use in their culture systems, and to evaluate reproducibility between different lots of FBS for a given set of experimental conditions. This potential for variability is further aggravated by the fact that suppliers neither guarantee permanent inventory nor the reproducibility of their product, although certain minimal serum assurances may be provided [Rolleston, 1999].

Several factors must be considered for explanation of the presence of inorganic crystalline material in FBS—a product subjected to several ultra-filtration steps before packaging. Supersaturation of calcium and oxalate levels in FBS with respect to the COD mineral phase, together with other physico-chemical parameters of the fluid phase, may partly explain the presence of crystals in FBS. The constituents of any given lot of FBS will likely show variation based on the bovine diet, the time of year and the locations from which the product was collected, and storage conditions are known to affect the preservation and activity of FBS. CaOx crystals are widely distributed in higher plant families where they play a calcium-sequestering and protective role, and this crystalline calcium can represent as much as 90% of total plant calcium [Webb, 1999; Franceschi and Nakata, 2005]. Plants abundant in North America, such as greasewood (*Sarcobatus vermiculatus*) and halogeton (*Halogeton glomeratus*), are rich in calcium oxalates and their abundant ingestion by grazing livestock can lead to oxalate poisoning causing kidney disease and failure from renal precipitation of calcium oxalate [Knight and Walter, 2003].

Another possible explanation for crystalline material appearing in FBS could be that suppliers might add undisclosed preservatives (as a proprietary processing method for FBS) such as ethylene glycol to the serum; ethylene glycol being a common additive for low-temperature preservation of biological samples. Moreover, ethylene glycol is used in the production of polyethylene terephthalate commonly employed in the manufacture of plastic bottles in which FBS is packaged. Leaching of ethylene glycol from these containers has been documented in some circumstances [Kashtock and Breder, 1980], indicating that the containers themselves may be a source of uncharacterized chemical constituents arriving at a late stage of packaging of the serum. Physiologically in vivo, the end metabolite of accidental (or experimental, in animal models) ethylene glycol ingestion is oxalic acid which can precipitate as CaOx in different tissues, especially in the kidney [McMartin and Wallace, 2005]. Thus, enzymes and/or other reactants in the FBS may interact with polyethylene terephthalate (or other contaminants), or with oxalic acid, to generate byproducts that may favor CaOx crystallization processes.

Another possible explanation for crystalline material in FBS is based on the fact that nanoscale amorphous precipitates and other complexed precursors existing in liquid FBS (like calciprotein particles in circulating plasma in vivo [Heiss et al., 2003]) might traverse the ultra-filtration units used in the purification process. Nanoscopic pathways to crystallization in non-living systems, and implications for mineralization, are discussed by Navrotsky [2004]. In our study, the estimated number of crystals from different bottles (from different suppliers) showed a wide range of values, which in turn was likewise reflected in the oxalate and calcium values determined chemically from crystals harvested from FBS. Crystals with morphologies differing from COD were sporadically isolated from FBS. Since COD crystals can convert with time and under other circumstances to the more energetically stable COM form of CaOx, we decided to evaluate both types of crystals in our experiments. COD crystals were predominantly present, compared to COM crystals, in the vast majority ($\sim$90%) of the FBS bottles we screened, indicating that the FBS milieu (including its proteins, pH, salt concentrations and other physico-chemical parameters), all favor the formation and stabilization of COD crystals over COM.

Surface roughness and rounded edges of the crystals, as seen in our study, can be explained by the influence of proteins on crystal growth and/or partial dissolution. Time of storage, serum freezing and thawing, and protein concentration are some of the parameters that might affect protein binding to the crystals. Proteins—well-known regulators of crystal growth—are present in FBS in a wide range of concentrations, and therein may facilitate or inhibit crystal formation. Although many users aliquot and freeze their sera to avoid changes to proteins associated with multiple freeze–thaw

cycles of a central batch, if this is not done, cycling temperature and phase changes may cause gradients of proteins and salts that facilitate crystal deposition. One of the most abundant proteins in serum having the potential to interfere with CaOx crystallization is albumin; its concentration in FBS has been reported to be 1.55 ± 0.63 g/dl [Honn et al., 1975]. In urine, albumin has been reported to promote COD crystallization as a protective mechanism that prevents stone formation by inhibiting larger crystal formation and aggregation [Cerini et al., 1999]. In FBS, albumin may have a similar function in favoring the formation of COD. Proteins present in kidney stone matrix [McKee et al., 1995], such as osteopontin and albumin, are present in FBS, and together with other unidentified proteins may be implicated in the mechanism by which CaOx forms in FBS. Other proteins with the potential to influence crystallization of CaOx and calcium-phosphate in urine are Tamm-Horsfall protein, nephrocalcin, osteopontin, calprotectin and urinary prothrombin fragment-1 [El-Shall et al., 2004]. In plasma, circulating, fetuin-mineral complexes correlate with artery calcification induced by vitamin D treatment in rats [Price et al., 2004]. They proposed, along with others [Schafer et al., 2003], that fetuin-A plays a role in vascular calcification in patients with chronic kidney disease where the levels and forms of calcium and phosphate are regulated by circulating protein inhibitors of mineralization [Ketteler et al., 2002; Moe and Chen, 2004]. Our results showing the association of fetuin-A with CaOx crystals collected from FBS likewise suggest a potential role for fetuin-A in regulating crystal formation in this commercially available, fluid biological product.

While generally similar, we observed some differences in the electrophoretic profiles of proteins eluted from crystals harvested from FBS compared to those proteins binding to synthetic forms of CaOx (COD and COM) when analyzed by SDS–PAGE. These results agree with other studies showing that the interaction of the two different forms of oxalate (COM and COD) with proteins is probably nonspecific [Walton et al., 2005], with protein binding likely occurring on multiple crystallographic faces of CaOx. Differences in serum-protein binding between FBS and synthetic crystals might also be attributable to the differing biochemical environments in which the crystals normally bind serum proteins versus the conditions used in the present study for the in vitro binding experiments using synthetic CaOx. More specifically, a preferential association of OPN with COD crystals compared to COM crystals has been recently reported [Ryall et al., 2005]. Here, we also demonstrate the association of OPN either with crystals harvested from FBS or with synthetic crystals, and also show preferential OPN binding to COD.

In the present study, we have shown cellular uptake of CaOx crystals by phagocytosis in both J744.A1 macrophages and in NIH/3T3 fibroblasts. It is well known that in response to crystal binding and phagocytosis, macrophages release inflammatory cytokines such as tumor necrosis factor and interleukin-6 into the culture medium [de Water et al., 2001]. Similarly, renal epithelial cells show increased expression of monocyte chemoattractant protein-1 when exposed to crystals of CaOx or calcium phosphate [Umekawa et al., 2003]. Koul et al. [2002] demonstrated that renal epithelial cells exposed to CaOx crystals activate p38 MAP kinase whose activity is essential for the effects of oxalate crystals on re-initiation of DNA synthesis. In joints in vivo, the interaction between calcium-containing crystals and macrophages leads to the synthesis and release of matrix metallo-proteinases which results in degeneration of articulating joint tissues [Cheung, 2005].

Here we show that exposure of cells to CaOx causes changes in cell–cell and cell–surface adhesion. Several of the components involved in cell adhesion, such as talin, vinculin, alpha-actinin and protein kinases, are also present in the actin-driven phagocytic cup [Aderem and Underhill, 1999], and their pathways and interactions might be altered by the exposure of the cells to the relatively large, particulate crystals used in our cell culture experiments. Cytoskeletal changes after exposure to crystals is consistent with a report by [Lieske et al., 1992] who, using data from MDCK renal epithelial cells, likewise suggested a role for actin during the process of CaOx phagocytosis in these cells.

Our results showing ROS induction in mouse macrophages are similar to those in studies by Thamiselvan et al., [Thamilselvan et al., 2000] who reported that CaOx crystal-induced injury to LLC-PK and MDCK epithelial cells is

associated with the production of free radicals, lipid peroxidation and release of lactate dehydrogenase—events associated with cell toxicity and death. Finally, we demonstrated that induction of proliferation in CaOx-treated cells is time-dependent, a finding in agreement with data from Lieske et al. [1994], who showed induction of cell proliferation in renal epithelial cells after exposure to CaOx.

As a final point, since FBS is used in its 10% diluted (with media) and warmed form in standard cell culture experiments, and dissolution of crystals occurs within 24 h, calcium concentrations can fluctuate widely when FBS containing COD crystals is used; even more so when fresh, FBS-containing media is regularly exchanged as is often done in longer-term experiments. Likewise, in the many laboratory assays that take place within a 24 h period, calcium release from the crystals may affect experimental outcomes to a significant but varying degree. In conclusion, these observations indicate that caution should be exercised when performing cell culture experiments where particulate materials and variable calcium and oxalate concentrations might affect experimental outcomes.

ACKNOWLEDGMENTS

The authors thank Line Mongeon for help with the scanning electron microscopy. Crystal phagocytosis studies on primary mouse macrophages was performed in the laboratory of Dr. Jaro Sodek (University of Toronto) with the assistance of Manju Bansal and Anil Bansal. This work was supported by a grant to MDM from the Canadian Institutes of Health Research (CIHR). MDM is a scholar of the Fonds de la recherche en santé du Québec, and a member of the McGill Centre for Bone and Periodontal Research, the McGill Centre for Biorecognition and Biosensors, and the McGill Institute for Advanced Materials. YC is a student scholar of the CIHR Training Program in Skeletal Health Research.

REFERENCES

Aderem A, Underhill DM. 1999. Mechanisms of phagocytosis in macrophages. Annu Rev Immunol 17:593–623.

Akbarieh M, Dubuc B, Tawashi R. 1987. Surface studies of calcium oxalate dihydrate single crystals during dissolution in the presence of urine. Scanning Microsc 1:1397–1403.

Bautista DS, Denstedt J, Chambers AF, Harris JF. 1996. Low-molecular-weight variants of osteopontin generated by serine proteinases in urine of patients with kidney stones. J Cell Biochem 61:402–409.

Belliveau J, Griffin H. 2001. The solubility of calcium oxalate in tissue culture media. Anal Biochem 291: 69–73.

Bratosin D, Mitrofan L, Palii C, Estaquier J, Montreuil J. 2005. Novel fluorescence assay using calcein-AM for the determination of human erythrocyte viability and aging. Cytometry A 66:78–84.

Burns JR, Finlayson B. 1980. Changes in calcium oxalate crystal, morphology as a function of concentration. Invest Urol 18:174–177.

Cerini C, Geider S, Dussol B, Hennequin C, Daudon M, Veesler S, Nitsche S, Boistelle R, Berthezene P, Dupuy P, Vazi A, Berland Y, Dagorn JC, Verdier JM. 1999. Nucleation of calcium oxalate crystals by albumin: Involvement in the prevention of stone formation. Kidney Int 55: 1776–1786.

Cheung HS. 2005. Biologic effects of calcium-containing crystals. Curr Opin Rheumatol 17:336–340.

Chiriboga J. 1963. Some properties of an oxalic oxidase purified from barley seedlings. Biochem Biophys Res Commun 11:277–282.

de Water R, Leenen PJ, Noordermeer C, Nigg AL, Houtsmuller AB, Kok DJ, Schroder FH. 2001. Cytokine production induced by binding and processing of calcium oxalate crystals in cultured macrophages. Am J Kidney Dis 38:331–338.

Elliot JS, Rabinowitz IN. 1980. Calcium oxalate crystalluria: Crystal size in urine. J Urol 123:324–327.

El-Shall H, Jeon J-H, Abdel-Aal EA, Khan S, Gower L, Rabinovich Y. 2004. A study of primary nucleation of calcium oxalate monohydrate. II. Effect of urinary species. Cryst Res Technol 39:222–229.

Finklea HO, Hanshew DD. 1992. Electron-transfer kinetics in organized thiol monolayers with attached pentaammine(pyridine)ruthenium redox centers. J Am Chem Soc 114:3173–3181.

Franceschi RT, Iyer BS. 1992. Relationship between collagen synthesis and expression of the osteoblast phenotype in MC3T3-E1 cells. J Bone Miner Res 7:235–246.

Franceschi VR, Nakata PA. 2005. Calcium oxalate in plants: Formation and Function. Annu Rev Plant Biol 56:41–71.

Greene EL, Farell G, Yu S, Matthews T, Kumar V, Lieske JC. 2005. Renal cell adaptation to oxalate. Urol Res 33: 340–348.

Hassoun EA, Wang X. 1999. Time- and concentration-dependent production of superoxide anion, nitric oxide, DNA damage and cellular death by ricin in the J774A.1 macrophage cells. J Biochem Mol Toxicol 13:179–185.

Heiss A, DuChesne A, Denecke B, Grotzinger J, Yamamoto K, Renne T, Jahnen-Dechent W. 2003. Structural basis of calcification inhibition by alpha 2-HS glycoprotein/fetuin-A. Formation of colloidal calciprotein particles. J Biol Chem 278:13333–13341.

Honn KV, Singley JA, Chavin W. 1975. Fetal bovine serum: A multivariate standard. Proc Soc Exp Biol Med 149: 344–347.

Kashtock M, Breder CV. 1980. Migration of ethylene glycol from polyethylene terephthalate bottles into 3% acetic acid. J Assoc Off Anal Chem 63:168–172.

Ketteler M, Vermeer C, Wanner C, Westenfeld R, Jahnen-Dechent W, Floege J. 2002. Novel insights into uremic vascular calcification: Role of matrix Gla protein and alpha-2-Heremans Schmid glycoprotein/fetuin. Blood Purif 20:473–476.

Khan SR. 2004. Role of renal epithelial cells in the initiation of calcium oxalate stones. Nephron Exp Nephrol 98:e55–e60.

Knight AP, Walter RG. 2003. A guide to plant poisoning of animals in North America. Ithaca: Teton NewMedia.

Konya E, Umekawa T, Iguchi M, Kurita T. 2003. The role of osteopontin on calcium oxalate crystal formation. Eur Urol 43:564–571.

Koul HK, Menon M, Chaturvedi LS, Koul S, Sekhon A, Bhandari A, Huang M. 2002. COM crystals activate the p38 mitogen-activated protein kinase signal transduction pathway in renal epithelial cells. J Biol Chem 277: 36845–36852.

Lasaga AC. 1998. Theory of crystals growth and dissolution. Kinetic theory in the earth sciences. Princenton: Princenton University Press.

Lepage L, Tawashi R. 1982. Growth and characterization of calcium oxalate dihydrate crystals (Weddellite). J Pharm Sci 71:1059–1062.

Lieske JC, Walsh-Reitz MM, Toback FG. 1992. Calcium oxalate monohydrate crystals are endocytosed by renal epithelial cells and induce proliferation. Am J Physiol 262:F622–F630.

Lieske JC, Swift H, Martin T, Patterson B, Toback FG. 1994. Renal epithelial cells rapidly bind and internalize calcium oxalate monohydrate crystals. Proc Natl Acad Sci USA 91:6987–6991.

Marsh ME, Munne AM, Vogel JJ, Cui Y, Franceschi RT. 1995. Mineralization of bone-like extracellular matrix in the absence of functional osteoblasts. J Bone Miner Res 10:1635–1643.

McKee MD, Nanci A, Khan SR. 1995. Ultrastructural immunodetection of osteopontin and osteocalcin as major matrix components of renal calculi. J Bone Miner Res 10:1913–1929.

McMartin KE, Wallace KB. 2005. Calcium oxalate monohydrate, a metabolite of ethylene glycol, is toxic for rat renal mitochondrial function. Toxicol Sci 84:195–200.

Moe SM, Chen NX. 2004. Pathophysiology of vascular calcification in chronic kidney disease. Circ Res 95:560–567.

Navrotsky A. 2004. Energetic clues to pathways to biomineralization: Precursors, clusters, and nanoparticles. Proc Natl Acad Sci USA 101:12096–12101.

Olton D, Li J, Wilson ME, Rogers T, Close J, Huang L, Kumta PN, Sfeir C. 2007. Nanostructured calcium phosphates (NanoCaPs) for non-viral gene delivery: Influence of the synthesis parameters on transfection efficiency. Biomaterials 28:1267–1279.

Price PA, Thomas GR, Pardini AW, Figueira WF, Caputo JM, Williamson MK. 2002. Discovery of a high molecular weight complex of calcium, phosphate, fetuin, and matrix gamma-carboxyglutamic acid protein in the serum of etidronate-treated rats. J Biol Chem 277:3926–3934.

Price PA, Williamson MK, Nguyen TM, Than TN. 2004. Serum levels of the fetuin-mineral complex correlate with artery calcification in the rat. J Biol Chem 279: 1594–1600.

Rolleston WB. 1999. Bovine serum: Reducing the variables through the use of donor herds. Dev Biol Stand 99:79–86.

Ryall RL. 2004. Macromolecules and urolithiasis: Parallels and paradoxes. Nephron Physiol 98:37–42.

Ryall RL, Chauvet MC, Grover PK. 2005. Intracrystalline proteins and urolithiasis: A comparison of the protein content and ultrastructure of urinary calcium oxalate monohydrate and dihydrate crystals. BJU Int 96:654–663.

Schafer C, Heiss A, Schwarz A, Westenfeld R, Ketteler M, Floege J, Muller-Esterl W, Schinke T, Jahnen-Dechent W. 2003. The serum protein alpha 2-Heremans-Schmid glycoprotein/fetuin-A is a systemically acting inhibitor of ectopic calcification. J Clin Invest 112:357–366.

Schinke T, Amendt C, Trindl A, Poschke O, Muller-Esterl W, Jahnen-Dechent W. 1996. The serum protein alpha2-HS glycoprotein/fetuin inhibits apatite formation in vitro and in mineralizing calvaria cells. A possible role in mineralization and calcium homeostasis. J Biol Chem 271:20789–20796.

Sorensen ES, Petersen TE. 1993. Phosphorylation, glycosylation and amino acid sequence of component PP3 from the proteose peptone fraction of bovine milk. J Dairy Res 60:535–542.

Staines D, Price P. 2003. Managing serum requirements for cell culture: GIBCO cell culture. pp 1–6

Thamilselvan S, Byer KJ, Hackett RL, Khan SR. 2000. Free radical scavengers, catalase and superoxide dismutase provide protection from oxalate-associated injury to LLC-PK1 and MDCK cells. J Urol 164:224–229.

Thrall MA, Dial SM, Winder DR. 1985. Identification of calcium oxalate monohydrate crystals by X-ray diffraction in urine of ethylene glycol-intoxicated dogs. Vet Pathol 22:625–628.

Umekawa T, Chegini N, Khan SR. 2003. Increased expression of monocyte chemoattractant protein-1 (MCP-1) by renal epithelial cells in culture on exposure to calcium oxalate, phosphate and uric acid crystals. Nephrol Dial Transplant 18:664–669.

Walton RC, Kavanagh JP, Heywood BR, Rao PN. 2005. The association of different urinary proteins with calcium oxalate hydromorphs. Evidence for non-specific interactions. Biochim Biophys Acta 1723:175–183.

Webb MA. 1999. Cell-mediated crystallization of calcium oxalate in plants. Plant Cell 11:751–761.